Journal of Fluorine Chemistry 197 (2017) 118–133

Contents lists available at ScienceDirect

Journal of Fluorine Chemistry

journal homepage: www.elsevier.com/locate/fluor

A computational study of SF_5-substituted carbocations

Gabriela L. Borosky[a,*], Kenneth K. Laali[b,*]

[a] INFIQC, CONICET and Departamento de Química Teórica y Computacional, Facultad de Ciencias Químicas, Universidad Nacional de Córdoba, Ciudad Universitaria, Córdoba 5000, Argentina

[b] Department of Chemistry, University of North Florida, 1,UNF Drive, Jacksonville, FL, 32224, USA

ARTICLE INFO

Dedicated with great respect to the memory of Prof. George Olah.

Keywords:
The SF_5 group
Substituent effects
Carbocations
Charge delocalization modes
GIAO-DFT

ABSTRACT

The effect of the SF_5 group as a substituent on various classes of carbocation was probed computationally employing DFT to examine geometrical changes, relative energies, and charge delocalization modes. Relative electron withdrawing power of the SF_5 group was compared with CF_3, NO_2, CN, and SCF_3 through isodesmic reactions. NPA charge densities were employed to gauge the influence of SF_5 group on the charge delocalization modes in the carbocations.

1. Introduction

The pentafluorosulfanyl (SF_5) group is a sterically demanding, strongly electron-withdrawing moiety. Its introduction into organic compounds increases lipophilicity, raises thermal and hydrolytic stability, and increases density. With these favorable characteristics SF_5-organics are in high demand for application in material science, biology and drug discovery [1]. Synthetic efforts to widen the scope of the available SF_5 compounds and increase the number of SF_5-bearing small molecule building blocks have evolved steadily, and progress in the area has been summarized in recent reviews [1,2].

Table 1 provides a comparative sense of lipophilicity and electron-withdrawing power (Ar-X substituent constants) among fluorinated groups, alongside the nitro and cyano groups [3–5]. Lipophilicity index for SF_5 is surpassed only by SCF_3, while its electron-withdrawing power is only slightly lower than NO_2, but exceeds SCF_3 and OTf.

Competitive $[NO_2][BF_4]$ nitration reactions ($PhSF_5$ vs $PhCF_3$ and $PhSF_5$ vs $PhNO_2$) underscored the stronger deactivating power of SF_5 relative to CF_3, placing it on the same footing with NO_2 [6]. A similar trend was observed in vicarious nucleophilic substitution, where SF_5 group was shown to activate nitrobenzenes more strongly than CF_3 or CN groups [7].

Fig. 1 highlights some key building blocks and type of chemistries that have been employed to expand the scope of SF_5-containing small molecules. Electron withdrawing power of SF_5 was logically exploited to synthesize numerous new derivatives via S_NAr chemistry [8], while a host of other SF_5-aromatics are accessible via cross coupling, azo-coupling, homocoupling, dediazoniation, and click chemistry starting with SF_5-bearing diazonium salts [9]. The iodo-derivative SF_5-Ph-I synthesized via iodo-dediazoniation [9] enters into Sonogashira coupling with alkynes [9a]. Boronic esters are also accessible via the diazonium salts [10]. The *m*-nitro(pentafluorsulfanyl)benzene enters into a direct Pd-catalyzed arylation cross-coupling to produce SF_5-bearing biphenyls and terphenyls [11]. The *ortho*-SF_5-benzyne generated from the fluoro-derivative undergoes cycloaddition to form adducts via the Diels-Alder reaction [12], while aldol condensation of α-SF_5-acetates with aldehydes furnishes α-SF_5-substituted-α,β-unsaturated carbonyl derivatives that can be elaborated into SF_5-bearing heterocycles [13]. The highly novel SF_5−C≡C−CF_3 acts as a powerful dienophile in Diels-Alder reaction [14].

Collectively, these and other synthetic efforts have produced diverse groups of small molecules that could potentially serve as precursors to reactive intermediates, in particular carbocations/arenium ions and carbanions/Meisenheimer complexes for direct studies.

The role of CF_3 group as substituent on various classes of carbocations has been extensively studied [15], likewise many types of NO_2 and CN substituted carbocations have been generated and studied [15]. However, to the best of our knowledge, SF_5-substituted carbocations have remained elusive. The outcome of the solvolytic/dediazoniation reaction shown below (Fig. 2) [9], provides a cautionary note about possible oxidation of SF_5 in superacid media, suggesting the use of both mild superacids and low temperatures. There is literature precedent for the formation of R-SF_4^+ cations by fluoride ion abstraction with SbF_5 at low temperature [16].

* Corresponding authors.
E-mail addresses: gborosky@fcq.unc.edu.ar (G.L. Borosky), Kenneth.Laali@UNF.edu (K.K. Laali).

http://dx.doi.org/10.1016/j.jfluchem.2017.04.002
Received 28 February 2017; Received in revised form 31 March 2017; Accepted 1 April 2017
Available online 02 April 2017
0022-1139/

Table 1
Lipophilicity indices (octanol/water partition coefficient) and Substituent Constants.

X	SCF_3	SF_5	OCF_3	CF_3	OSO_2CF_3	SO_2CF_3	NO_2	CN
π_p	**1.44**	**1.23**	1.04	0.88		0.55	−0.28	
σ_{meta}	0.40	**0.61**	0.39	0.43	0.56	**0.83**	**0.71**	0.56
σ_{para}	0.50	**0.68**	0.35	0.54	0.53	**0.96**	**0.78**	**0.66**
σ^+(para)				0.61			0.79	0.66
σ^-(para)	0.64	**0.86**	0.27	0.65	0.49	**1.54**	**1.27**	**1.0**

In the present computational study we have examined different classes of SF_5-bearing carbocations. Relative energies, optimized geometries, charge delocalization modes, GIAO-NMR data, and isodesmic reactions were investigated to examine the effect of the SF_5 group as substituent, and its impact in comparison to CF_3 and NO_2 groups. It was hoped that these studies could assist future experimental stable ion work.

2. Computational procedures

Density functional theory (DFT) calculations were performed with the Gaussian 09 suite of programs [17]. Structures were fully optimized with the B3LYP functional [18] and the 6-311 + G(3df,2p) basis set. For comparison, additional computations were also carried out at the B3LYP/6-31 + G(df,p), MP2/6-311G(d,p), and B3LYP/aug-cc-pVTZ levels. Stationary points were characterized as minima (no imaginary frequencies) by harmonic vibrational frequency calculations. Natural bond orbital population analysis (NPA) was evaluated with the NBO program [19]. NMR chemical shifts were calculated by the GIAO (gauge independent atomic orbitals) method [20]. The ^{13}C, ^{15}N, and ^{19}F NMR chemical shifts were referenced to TMS, nitromethane, and $CFCl_3$, respectively. GIAO magnetic shielding tensors were 183.8 ppm for ^{13}C, and −153.2 ppm for ^{15}N, values related to the GIAO isotropic magnetic susceptibility. Magnetic shielding tensors for ^{19}F were 164.7 (B3LYP/6-311 + G(3df,2p)), 178.9 (B3LYP/6-31 + G(df,p)), and 208.9 (MP2/6-311G(d,p)). Solvation effects were included by means of polarized continuum model (IEFPCM) [21] energy minimizations in CH_2Cl_2 (dielectric constant ε = 8.93).

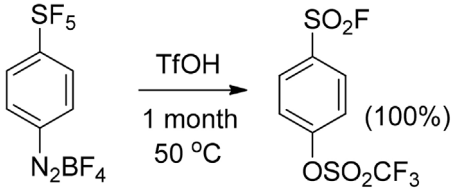

Fig. 2. Solvolysis of SF_5-diazonium in TfOH.

3. Results and discussion

The influence of electron withdrawing groups (SF_5, CF_3, NO_2, CN, SF_3, SCF_3) on the stability and properties of several types of carbocations was evaluated by DFT computations. Calculations were performed in the gas phase and in CH_2Cl_2 as solvent. Substituent effect analysis are described by carbocation type.

3.1. Benzenium ions

The molecular structures of several benzenium ions generated by protonation at the *o*-, *m*-, and *p*- positions of monosubstituted benzenes were characterized by DFT calculations. For each substituent, the optimized geometrical parameters and electronic properties were examined to determine the influence of the electronegative groups on the relative stabilities of the *o*-, *m*-, and *p*-protonated isomers. Bond distances are illustrated in Fig. 3, NPA charge densities are shown in Figs. 4 and 5, whereas GIAO-NMR chemical shifts are displayed in Fig. 6.

With the strongly withdrawing $-NO_2$, $-SF_5$, and $-CF_3$ groups, the stability order was *m*- > *o*- ≈ *p*-, as expected according to the known

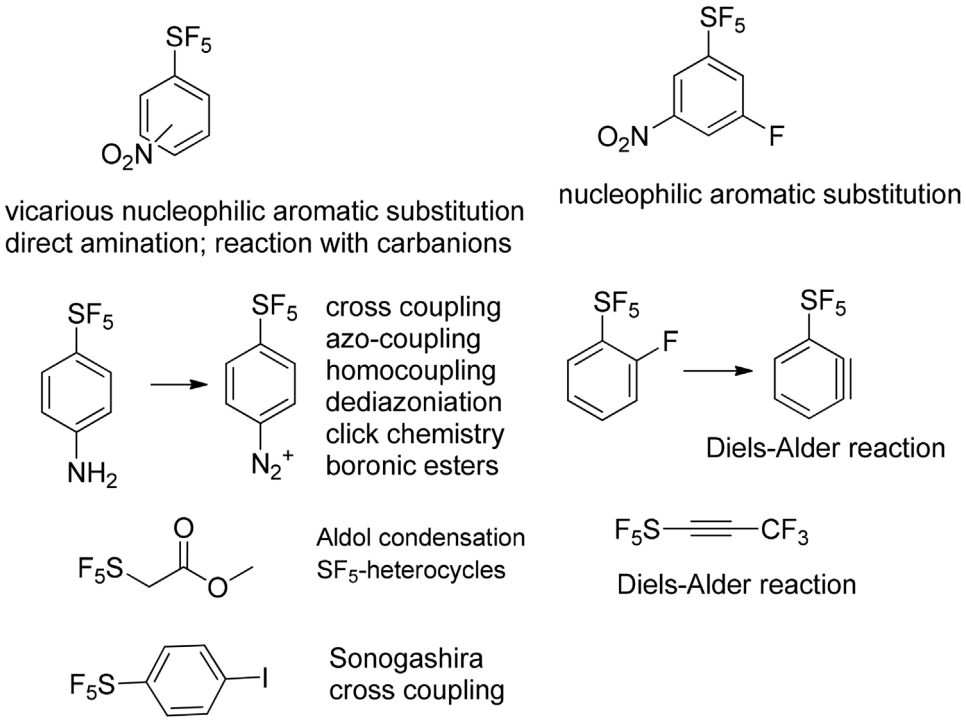

Fig. 1. Important building blocks and chemistries.

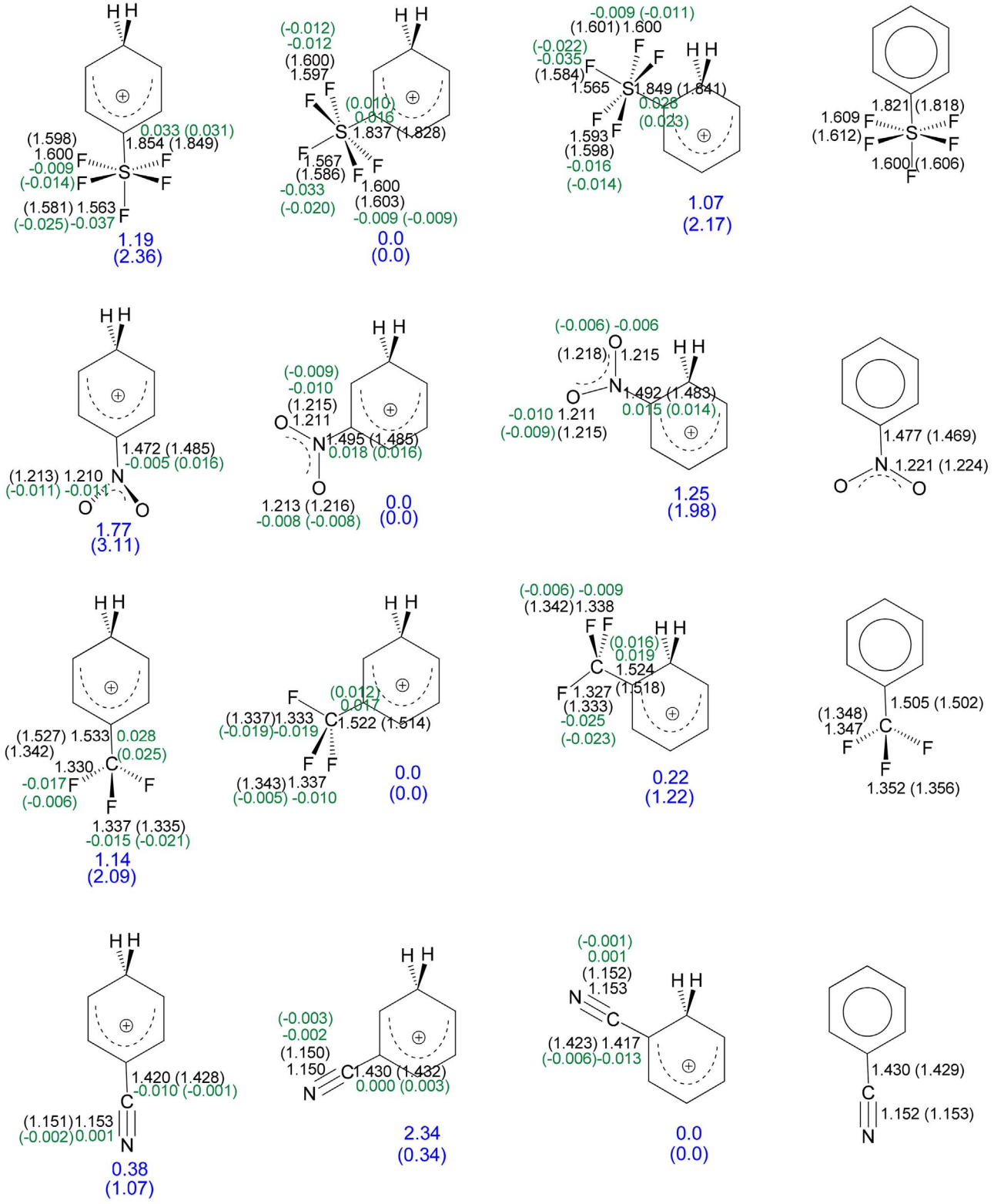

Fig. 3. Optimized bond lengths (Å), differences in bond distances (cation – neutral molecule; Å, in green), and relative energies (kcal/mol, in blue) for benzenium ions in gas phase. Results in CH_2Cl_2 in parenthesis. (For interpretation of the references to colour in this figure legend, the reader is referred to the web version of this article.)

m-directing effect of electronegative substituents in electrophilic aromatic substitution [22]. Solvation increased the differences in relative stability between isomers. These substituents developed the highest positive charge density relative to the neutral compounds when located at the *p*-position (Figs. 4 and 5, and Table 2), a destabilizing influence for such electron withdrawing groups. Computed ^{13}C NMR chemical shifts (Fig. 6) show the order of deshielding of the *ipso* carbon SF_5 > CF_3 > CN, and this trend is observed for all isomers.

For the nitro carbocations, acquisition of positive charge by the substituent was also evidenced by the increase in the C—N bond distance along with shortening of the N—O bonds (Fig. 3 and Table 2). It is interesting to note that in the *o*- and *m*-isomers the

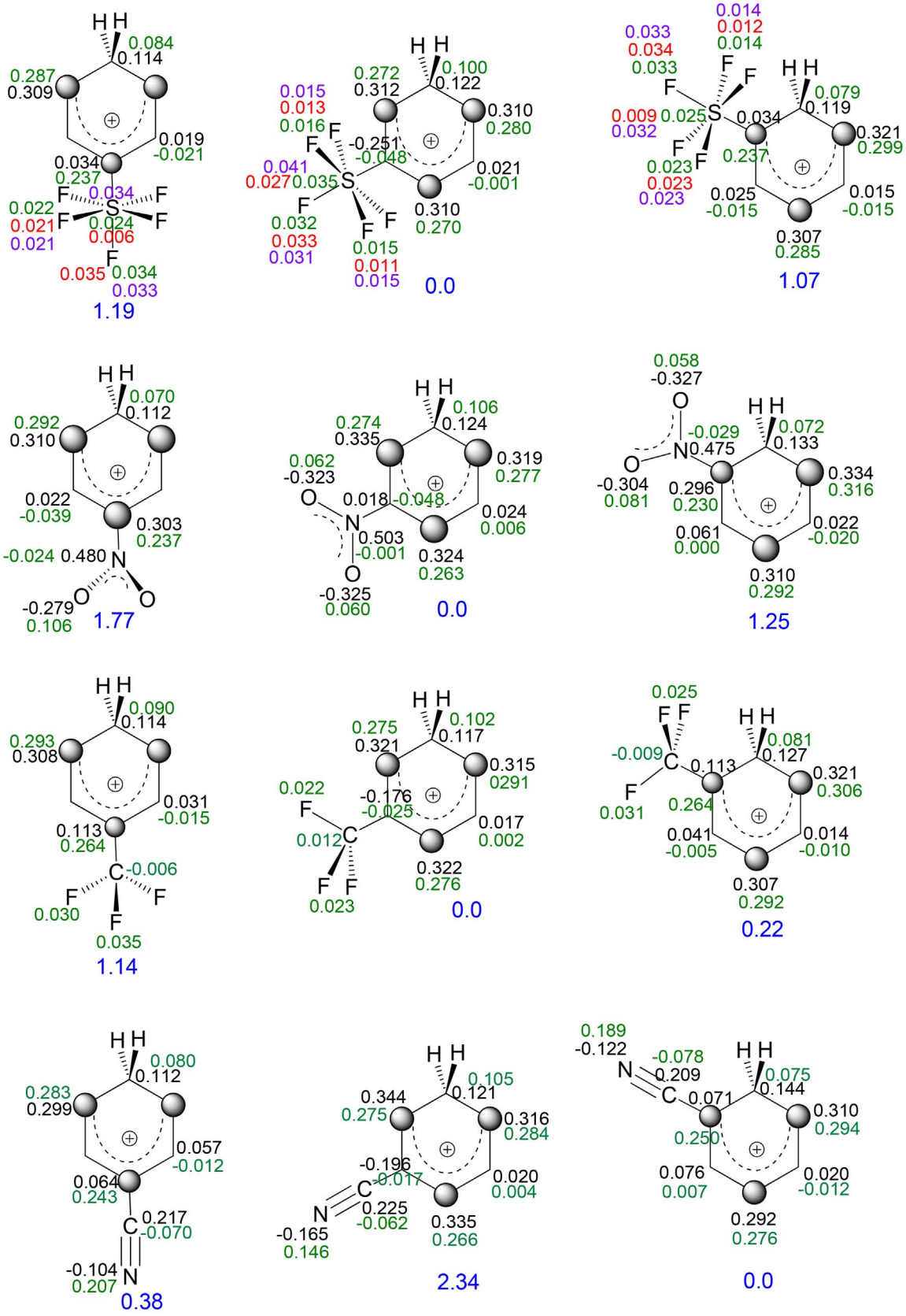

Fig. 4. NPA charges, Δcharges (cation – neutral, in green), and relative energies (kcal/mol, in blue) at the B3LYP/6-311 + G(3df,2p) level for the benzenium ions in the gas phase (dark circles signify positions with high positive charge); Δcharges at the MP2/6-311G(d,p) level in red, and at the B3LYP/6-31 + G(df,p) level in purple. (For interpretation of the references to colour in this figure legend, the reader is referred to the web version of this article.)

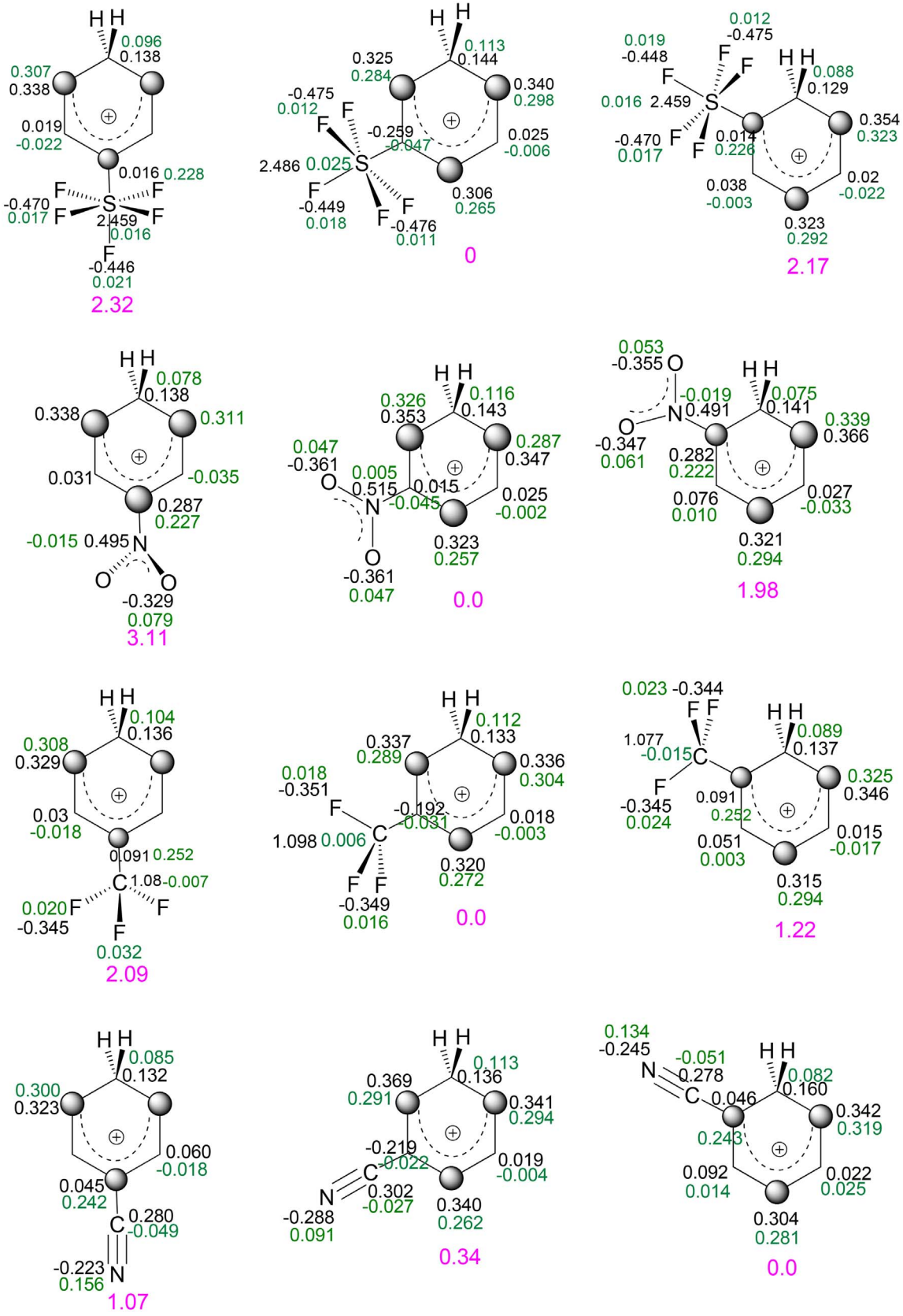

Fig. 5. NPA charges, Δcharges (cation – neutral, in green), and relative energies (kcal/mol, in pink) at the B3LYP/6-311 + G(3df,2p) level for the benzenium ions in CH_2Cl_2. (For interpretation of the references to colour in this figure legend, the reader is referred to the web version of this article.)

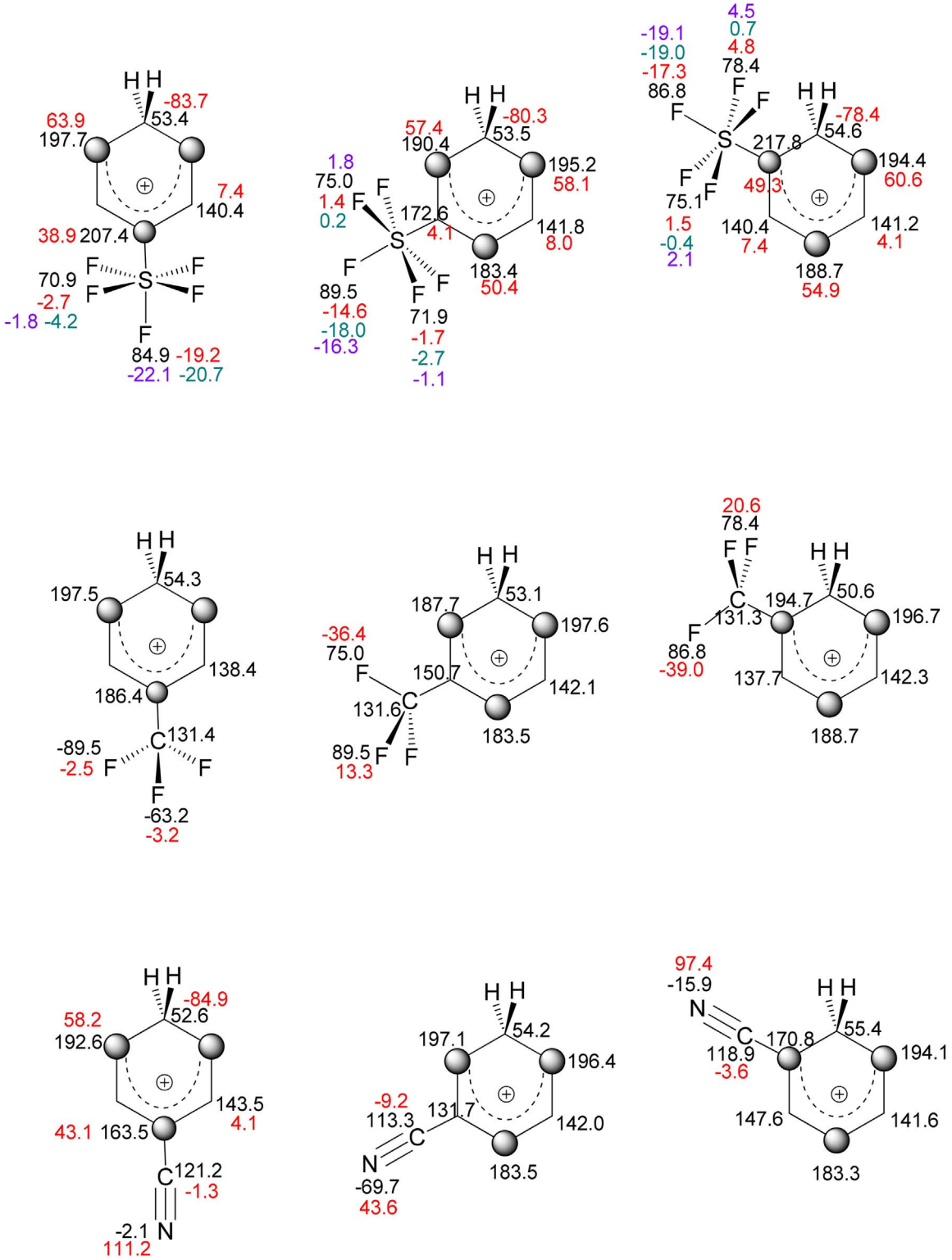

Fig. 6. GIAO-NMR chemical shifts and Δδ (cation – neutral, in red) for benzenium ions at the B3LYP/6-311 + G(3df,2p) level; Δδ at the MP2/6-311G(d,p) level in green, and at the B3LYP/6-31 + G(df,p) level in purple. (For interpretation of the references to colour in this figure legend, the reader is referred to the web version of this article.)

Table 2
Computed properties for the benzenium ions and benzylic cations.[a]

Substituent	Relative stability (kcal/mol)	Δcharge on substituent	Changes in bond lengths upon protonation (Å)		
$-NO_2$	*m*- 0.0 (0.0)	0.121 (0.099)	C–N	N–O	–
			0.018 (0.016)	−0.010 (−0.009)	–
	o- 1.25 (1.98)	0.110 (0.095)	0.015 (0.014)	−0.010 (−0.009)	–
	p- 1.77 (3.11)	0.188 (0.143)	−0.005 (0.016)	−0.011 (−0.011)	–
$-SF_5$	*m*- 0.0 (0.0)	0.129 (0.089)	C–S	$S\text{-}F_{eq}$	$S\text{-}F_{ax}$
			0.016 (0.010)	−0.012 (−0.012)	−0.033 (−0.020)
	o- 1.07 (2.17)	0.132 (0.093)	0.028 (0.023)	−0.016 (−0.014)	−0.035 (−0.022)
	p- 1.19 (2.36)	0.146 (0.105)	0.033 (0.031)	−0.009 (−0.014)	−0.037 (−0.025)
$-CF_3$	*m*- 0.0 (0.0)	0.080 (0.056)	C–C	C–F (2 bonds)	C–F (1 bond)
			0.017 (0.012)	−0.010 (−0.005)	−0.019 (−0.019)
	o- 0.22 (1.22)	0.072 (0.055)	0.019 (0.016)	−0.009 (−0.006)	−0.025 (−0.023)
	p- 1.14 (2.09)	0.089 (0.065)	0.028 (0.025)	−0.017 (−0.006)	−0.015 (−0.021)
−CN	*o*- 0.0 (0.0)	0.111 (0.083)	C–C	C–N	–
			−0.013 (−0.006)	0.001 (−0.001)	–
	p- 0.38 (1.07)	0.137 (0.107)	−0.010 (−0.001)	0.001 (−0.002)	–
	m- 2.34 (0.34)	0.084 (0.064)	0.000 (0.003)	−0.002 (−0.003)	–
$-SF_5$ (benzylic)	*m*- 0.0 (0.0)	0.122 (0.083)	C-S	$S\text{-}F_{eq}$	$S\text{-}F_{ax}$
			0.015 (0.007)	−0.012 (−0.010)	−0.031 (−0.018)
	p- 0.91 (1.59)	0.133 (0.094)	0.031 (0.028)	−0.014 (−0.012)	−0.033 (−0.022)
	o- 4.73 (6.52)	0.121 (0.090)	0.016 (0.010)	−0.017 (−0.015)	−0.032 (−0.022)

[a] Values in CH_2Cl_2 in parenthesis.

$-NO_2$ group was coplanar with the ring, while in the *p*-isomer it rotated, with the O–N–O forming a dihedral angle of 71 ° with the ring plane. This dihedral angle reduced to 46 ° in CH_2Cl_2.

The cations with fluorinated $-SF_5$ and $-CF_3$ substituents revealed loss of electron density at fluorine atoms. These observations were in correspondence with the increment of the C–S and C–CF_3 bond lengths along with the decrease in the S–F and C–F distances, indicating development of fluoronium ion character. This was especially noticeable for the axial fluorine of the $-SF_5$ group. However, GIAO-NMR ^{19}F Δδ chemical shifts showed erratic shielding and deshielding patterns upon protonation. In order to clarify this issue, further calculations were performed including *f*-functions (B3LYP/6-31 + G(df,p)), using a more extended basis set (B3LYP/aug-cc-pVTZ), and at the MP2/6-311G(d,p) level (Fig. 6). Nevertheless, no clear fluoronium character was revealed by inspecting the corresponding Δδ chemical shifts. According to important deviations from experimental values, extensive computations applying a considerable number of levels of theory have demonstrated that ^{19}F chemical shifts are very sensitive to the calculation method as well as the basis set [23]. Moreover, the chemical shifts of the fluorine nuclei attached to four- and six-coordinated sulfur atoms exhibited large differences between theoretical and experimental values and no suitable basis set could be found, even though large basis sets afforded proper S–F bond lengths and atomic charge values [24]. Taking this into account, only variations in bond distances and NPA charges were considered to deduce the existence of fluoronium character for every cation in the present study.

The protonated isomers of the disubstituted 1-SF_5-2-CF_3-benzene were also calculated to assess the relative effects of both fluorinated groups, but no preference for protonation of the position *meta* to the $-SF_5$ or the $-CF_3$ group was observed (Fig. 7). Considering the small difference in their relative energies it is quite likely that a mixture of the two isomeric benzenium ions would be formed in solution.

Among the cyano-substituted benzenium ions, the *ortho*-isomer was the most stable followed by *para* in the gas phase, whereas in DCM as solvent, the *meta*-isomer was almost as stable as the *ortho*. This substituent is apparently able to stabilize the positive charge by resonance, having an *ortho/para* directing effect in the gas phase. Natural bonding orbital (NBO) analysis revealed an overlap between the C–H bonds of the protonated carbocation and the C–CN π-system, especially for the *ortho*-isomer, an indication of hyperconjugation (Fig. 8). This effect diminished in the presence of a polar solvent (Fig. 8), leading to the usual *m*-directing effect.

3.2. Benzylic cations

Benzylic carbocations generated by ionization of alcohol precursors, substituted at the *o*-, *m*-, and *p*-positions, were examined as model systems to gauge substituent effects. Optimized structures and electron density properties were analyzed to study the effect of the $-SF_5$ group on the relative stabilities of the *o*-, *m*-, and *p*-protonated cations. Geometrical features are displayed in Fig. 9. NPA charge densities and GIAO-NMR chemical shifts are shown in Fig. 10. The results are summarized in Table 2.

The stability order of SF_5-benzyl cations was *m*- > *p*- > *o*-isomer, indicating regular *m*-directing effect of an electron withdrawing group. The *o*-derivative was further destabilized by steric interactions between the $-SF_5$ substituent and the proximate hydrogen of the benzylic carbon, as evidenced by distortion of the angles centered at the C–CH_2 atom (Fig. 9). Significant features in the optimized structures of the benzylic cations are shortening of the Ph–CH_2^+ bond, along with lengthening of the C–S bond, and shortening of the S–F bonds, particularly the axial one (Table 2). These changes appear more pronounced in the p-protonated isomer and reflect the familiar p-pi overlap, but presence of positive charge has a destabilizing effect on the SF_5 substituent, leading to C–S bond weakening that is compensated by fluorine back-bonding. Whereas computed ^{13}C NMR chemical shift for the benzylic cation is almost identical for the isomeric *p*-SF_5 and *m*-SF_5, it is more deshielded in the sterically crowded *o*-SF_5, providing a clear example for steric inhibition to delocalization. Relative deshielding at the *ipso* carbon is *p*-SF_5 > *o*-SF_5 > > *m*-SF_5, which seems to correlate

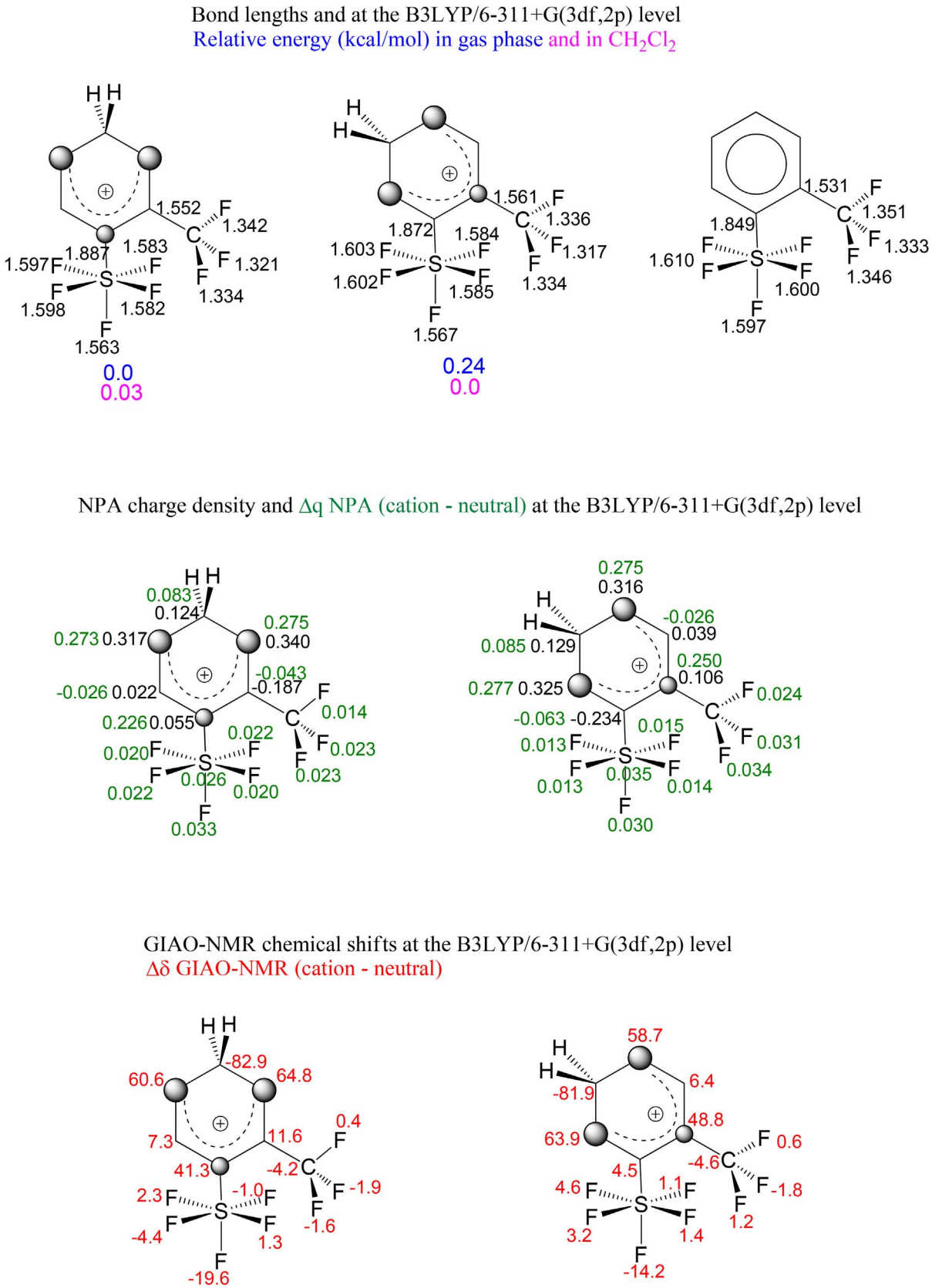

Fig. 7. Computed properties for the disubstituted benzenium ions.

with the order of C-SF_5 bond lengthening.

3.3. Benzoyl and thiobenzoyl cations

The *m*-substituted benzoyl and thiobenzoyl cations obtained by hydride loss from the corresponding aldehydes and thioaldehydes were considered as models and optimized to assess the effect of an electronegative group on the electron density distribution. NPA charge densities are illustrated in Fig. 11, while GIAO-NMR chemical shifts are shown in Fig. 12. Positive charge is delocalized *ortho/para*, and the inductive destabilization by the *meta* substituents does not appear to have a major effect, since no significant variations on charge densities are produced by the different substituents.

3.4. Allylic cations

Model allylic carbocations bearing SF_5, CF_3, and NO_2 substituents were examined and compared with the parent allyl cation. Their computed properties are described in Fig. 13. Only small variations in the bond distances are observed in the substituted allylic cations but NPA charges clearly reflect the charge destabilization effect of the substituents making allylic C-3 significantly more electrophilic. This tendency can be modulated via substitution at C-3. The computed ^{13}C chemical shift of the allylic C-1 changes from δ 243 (SF_5) to 228 (CF_3), and then to 186 ppm (NO_2), respectively.

3.5. Propargyl-Allenyl cations

The effect of the $-SF_5$ group attached to propargyl cations formed via ionization of the isomeric propargylic alcohols (A and D) were also examined (Fig. 14). Calculations at the B3LYP/6-311 + G(d,p) yielded almost the same results as B3LYP/6-311 + G(3df,2p) and B3LYP/aug-cc-pVTZ computations. The carbocation derived from ionization of the primary alcohol A is best described as a resonance hybrid of propargyl allenyl structure B/C. Fluoronium ion character in the hybrid cation is inferred according to lengthening of the C—S bond and shortening of the S—F bonds, especially the axial S—F. The carbocation derived from the secondary propargylic alcohol D exhibits shorter S—F and C—S bond. Geometrical changes and the GIAO-NMR data imply significant allenyl character (**E**/F) which is in concert with destabilizing/electron-withdrawing effect of SF_5.

3.6. Vinyl cations

The effect of the SF_5 substituent on the protonation site of a diarylacetylene (a) was studied (Fig. 15). The cationic carbon adopts sp-

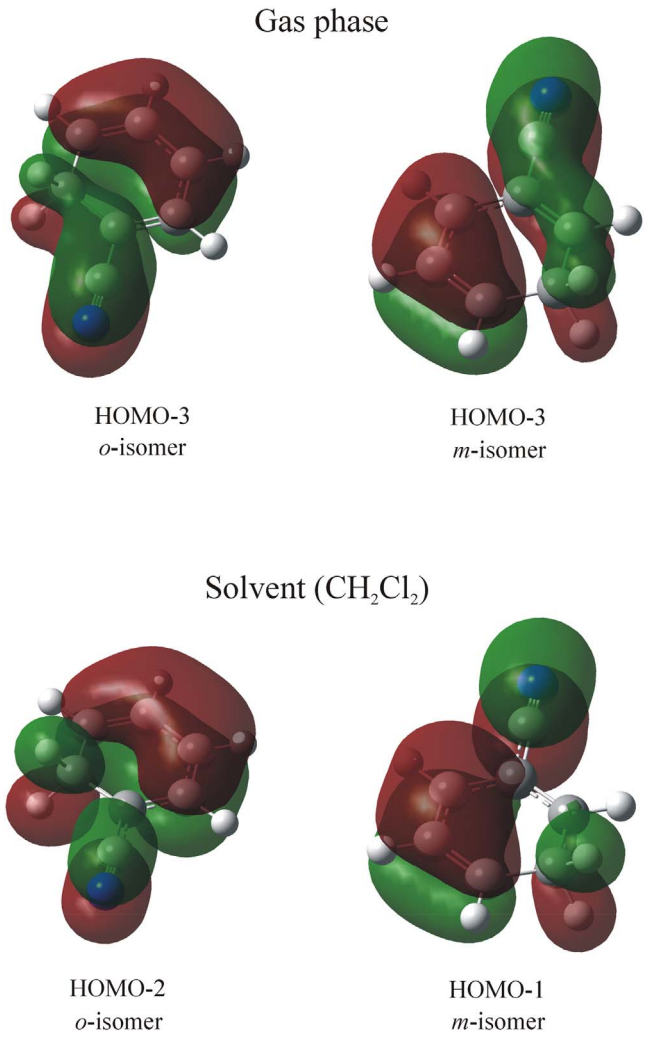

Fig. 8. NBO orbitals for the isomeric CN-substituted benzenium ions.

hybridization and, by resonance, the positive charge delocalizes into the attached aromatic group. The more stable carbocation (by over 4 kcal/mol) is the one with the sp-carbon attached to the phenyl ring (b), while the other isomer (c) is destabilized by the electron withdrawing influence of the *p*-SF_5-Ph substituent, as deduced by NPA charges and ^{13}C NMR shifts (Fig. 15). Fluoronium ion character in c is inferred in line with the features described above for the SF_5-bearing benzylic cations.

3.7. Isodesmic reactions

Calculations at the B3LYP/6-311 + G(3df,2p) level were performed with the aim to compare the effect of the $-SF_5$ group with other electron withdrawing substituents on different types of carbocations via hydride transfer reactions (Fig. 16). Slight differences in trends were observed between the gas phase and DCM. For reaction (1), $-SF_3$ and $-NO_2$ are not far behind $-SF_5$, and for reaction (2) hydride transfer becomes very slightly favorable with R = NO_2 or CN. For reaction (3) hydride abstraction from adamantane is most favorable with R = SF_5 followed by NO_2 in DCM, but the reverse order is observed in the gas phase.

4. Conclusions

The present computational study of various classes of SF_5-bearing carbocations has underscored the powerful electron-withdrawing effect of the pentafluorosulfanyl group. In concert with earlier data based on competitive reactions and substituent constants, the present study places SF_5 group in par with NO_2. Lengthening of the C—Si bond and shortening of the S—F bond along with development of positive charge (mainly at the axial fluorine) are consistent with onset of fluoronium ion character in SF_5-substituted benzenium and benzylic cations as well as in mesomeric propargyl/allenyl, and vinyl cations.

Through the present model computational study we have examined several classes of SF_5-carbocations. Their relative stability data, charge delocalization modes, and computed GIAO-NMR data, could serve as a guiding tool in future synthetic and experimental stable ion studies.

Acknowledgements

G.L.B gratefully acknowledges financial support from Consejo Nacional de Investigaciones Científicas y Técnicas (CONICET) and the Secretaría de Ciencia y Tecnología de la Universidad Nacional de Córdoba (Secyt-UNC).

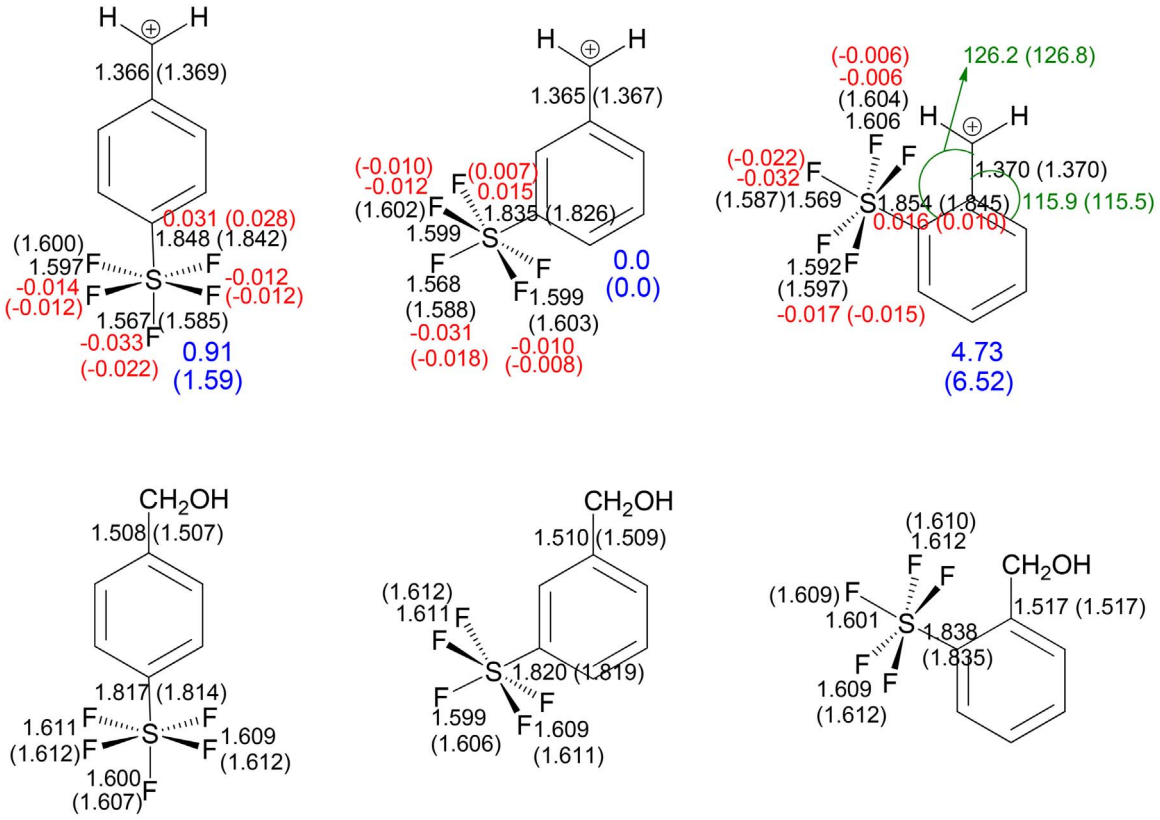

Fig. 9. Optimized bond lengths (Å) and angles (degrees, in green), and relative energies (kcal/mol, in blue) for the benzylic cations in gas phase. Differences in bond distances for cation – neutral molecule in red. Results in CH_2Cl_2 in parenthesis. (For interpretation of the references to colour in this figure legend, the reader is referred to the web version of this article.)

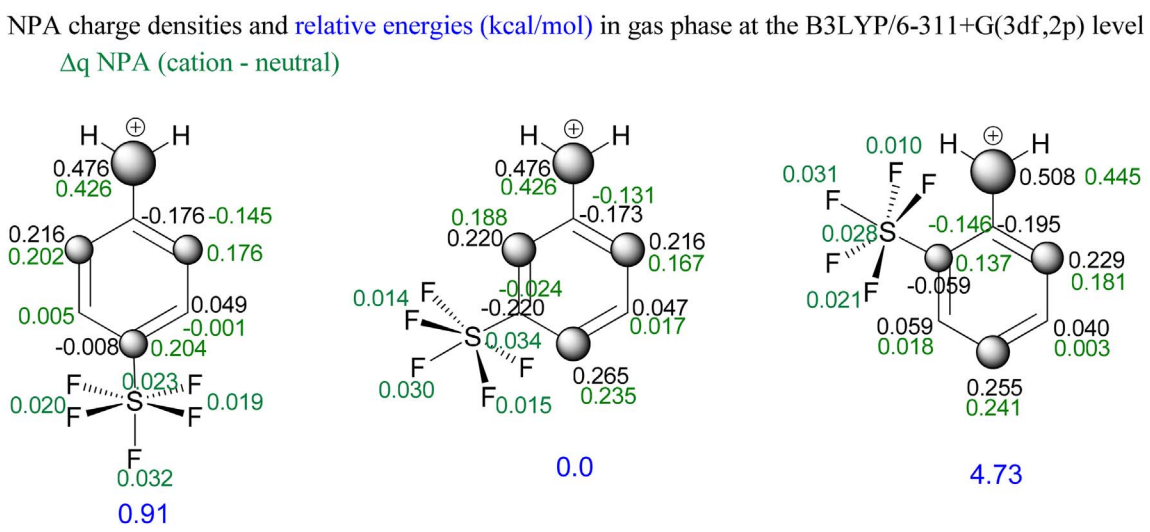

Fig. 10. NPA charges and GIAO-NMR chemical shifts for benzylic carbocations.

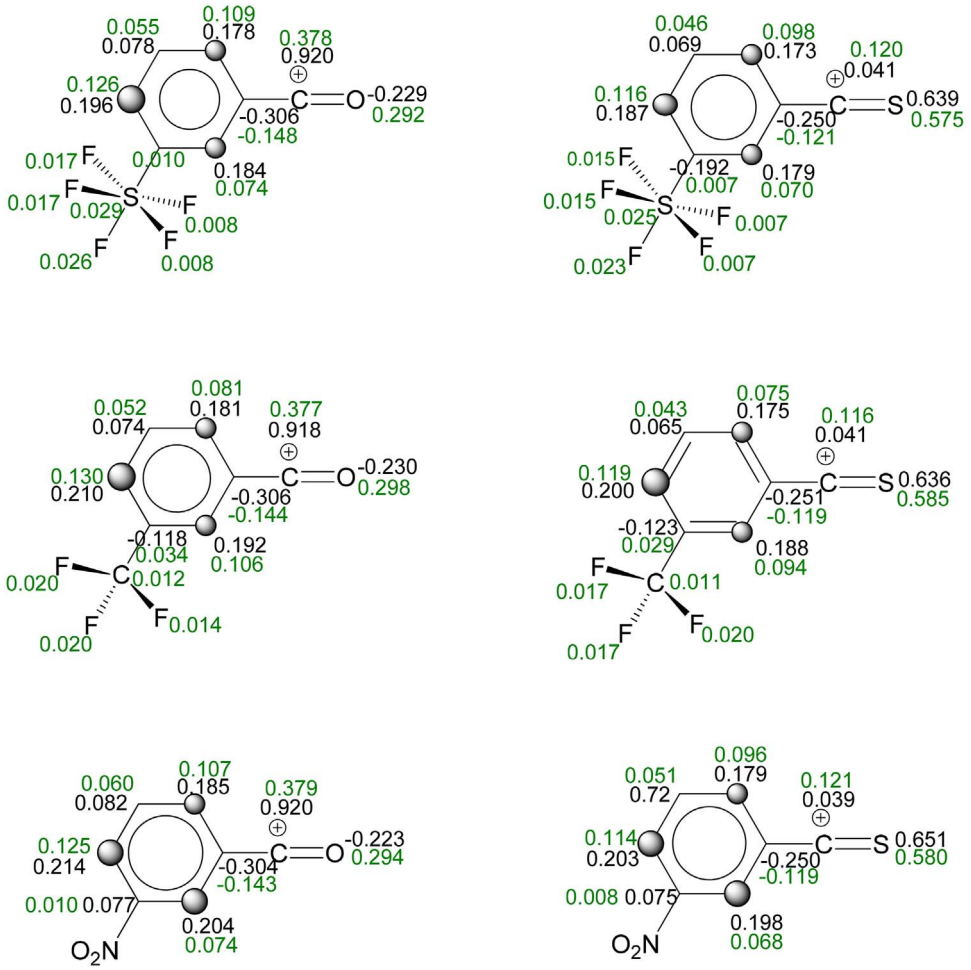

Fig. 11. NPA charges and Δcharges (cation – neutral, in green) for benzoyl and thiobenzoyl cations. (For interpretation of the references to colour in this figure legend, the reader is referred to the web version of this article.)

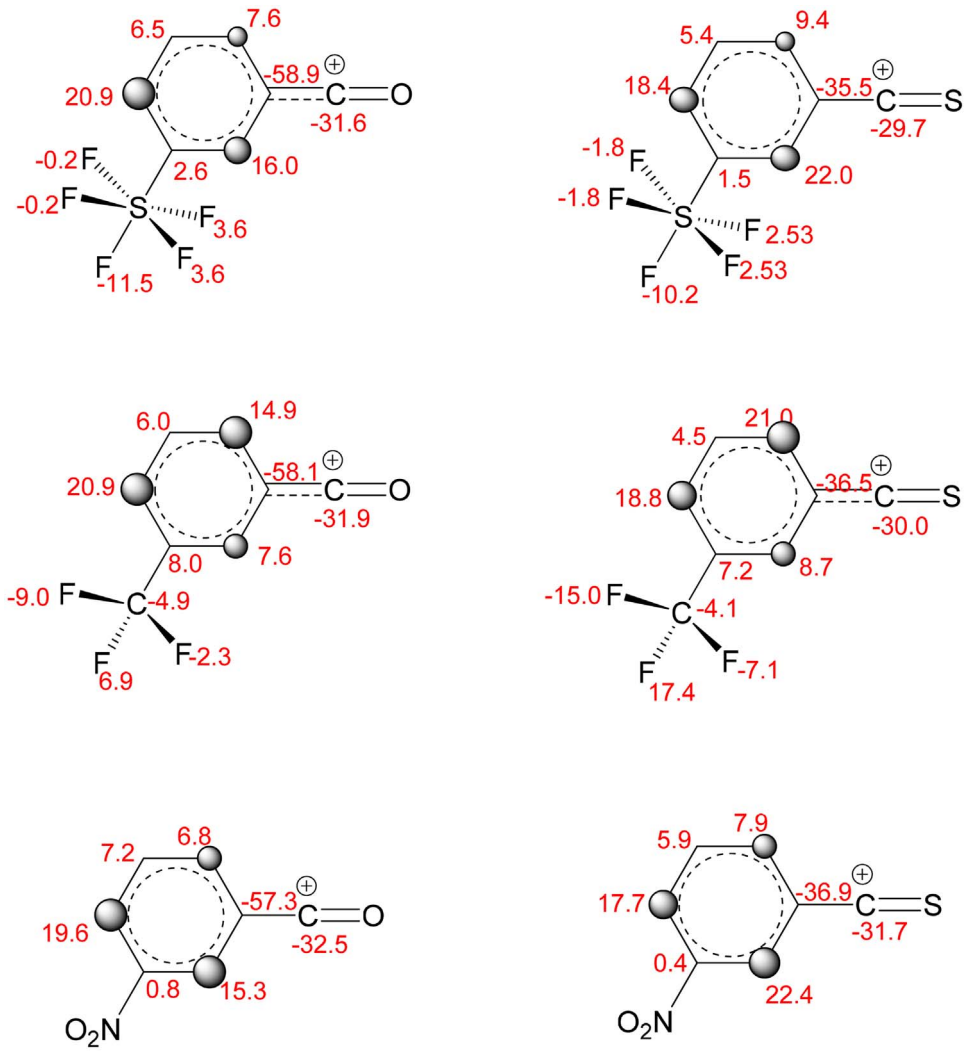

Fig. 12. Δδ GIAO-NMR chemical shifts (cation – neutral) for benzoyl and thiobenzoyl cations.

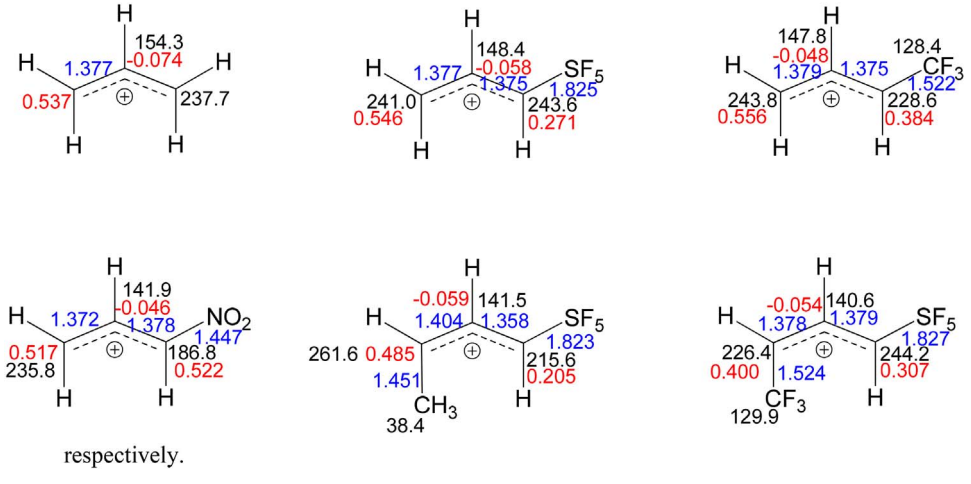

Fig. 13. Computed features for allylic cations: ^{13}C GIAO-NMR chemical shifts, NPA charge densities (in red), and bond distances (Å, in blue). (For interpretation of the references to colour in this figure legend, the reader is referred to the web version of this article.)

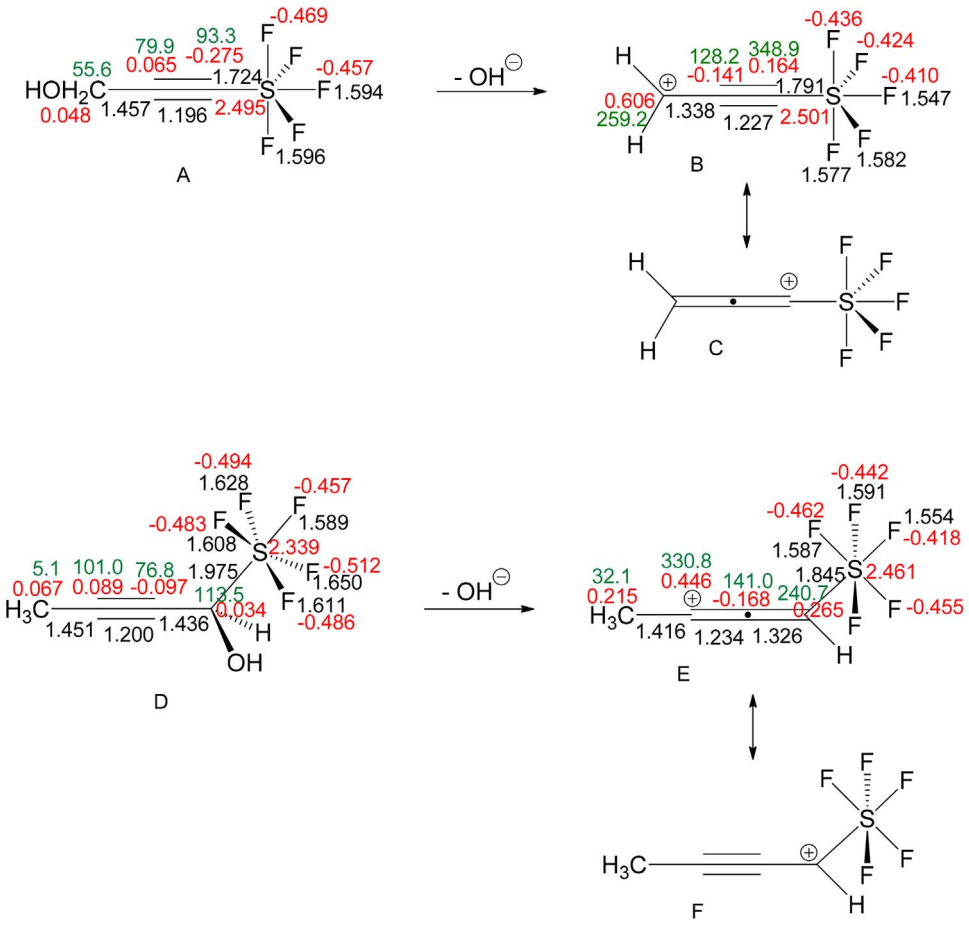

Fig. 14. Computed properties for the propargylic cations: bond distances (Å), NPA charge densities (in red), and ^{13}C GIAO-NMR chemical shifts (in green). (For interpretation of the references to colour in this figure legend, the reader is referred to the web version of this article.)

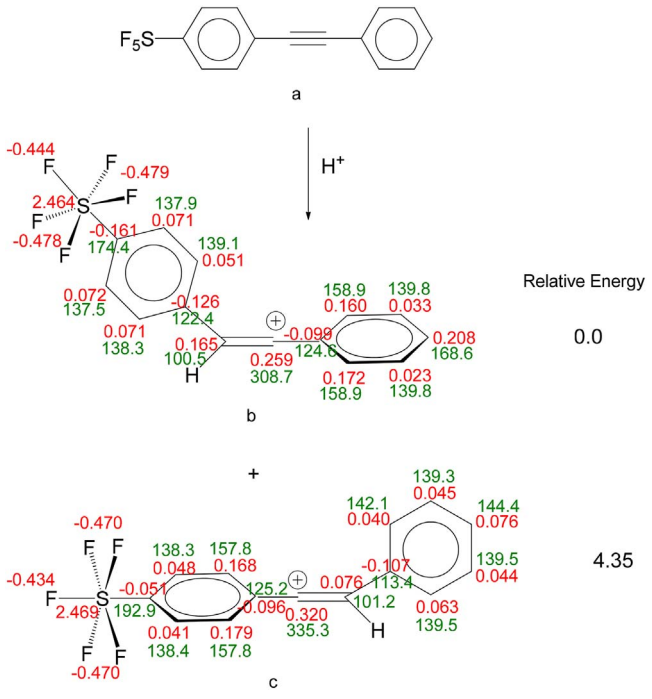

Fig. 15. Computed properties for the vinyl cations: relative energies (kcal/mol), NPA charge densities (in red), and 13C GIAO-NMR chemical shifts (in green). (For interpretation of the references to colour in this figure legend, the reader is referred to the web version of this article.)

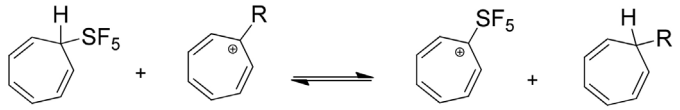

(1)

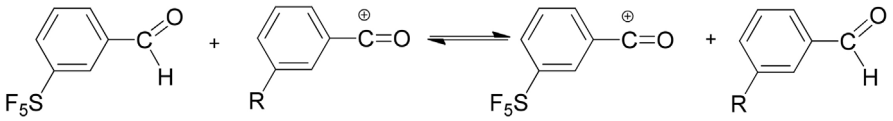

(2)

Reaction energy (kcal/mol) (CH_2Cl_2)

R	Reaction 1	Reaction 2
—CH_3	19.51 (16.96)	13.03 (9.16)
—SCF_3	11.28 (8.57)	3.51 (2.82)
—CN	2.77 (4.62)	-2.26 (0.18)
—CF_3	1.55 (2.19)	1.67 (2.24)
—SF_3	1.11 (0.20)	3.14 (1.64)
—NO_2	-1.03 (0.74)	-2.65 (-0.78)

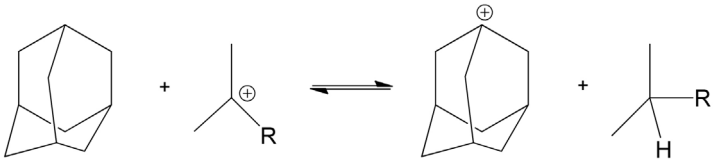

(3)

Reaction energy (kcal/mol)

R	Gas phase	CH_2Cl_2
—CH_3	-10.50	-2.85
—SCF_3	-9.98	-5.66
—CN	-40.44	-32.33
—CF_3	-44.25	-35.60
—SF_5	-46.60	-40.74
—NO_2	-47.25	-38.91

Fig. 16. Computed isodesmic reactions.

References

[1] S. Altomonte, M. Zanda, J. Fluor. Chem. 143 (2012) 57–93.
[2] (a) C.N. von Hahmann, P.R. Savoie, J.T. Welch, Curr. Org. Chem. 19 (2015) 1592–1618;
(b) P.R. Savoie, J.T. Welch, Chem. Rev. 115 (2015) 1130–1190.
[3] C. Hansch, R.M. Muir, T. Fujita, P.P. Maloney, F. Geiger, M. Streich, J. Am. Chem. Soc. 85 (1963) 2817–2824.
[4] C. Hansch, A. Leo, R.W. Taft, Chem. Rev. 91 (1991) 165–195.
[5] X.-H. Xu, K. Matsuzaki, N. Shibata, Chem. Rev. 115 (2015) 731–764.
[6] T. Okazaki, K.K. Laali, J. Fluor. Chem. 165 (2014) 96–100.
[7] P. Beier, Phosphorous Sulfur 192 (2017) 212–215.
[8] (a) P. Beier, T. Pastýříková, Beilstein J. Org. Chem. 9 (2013) 411–416;
(b) P. Beier, T. Pastýříková, G. Iakobson, J. Org. Chem. 76 (2011) 4781–4786;
(c) J. Ajenjo, M. Greenhall, C. Zarantonello, P. Beier, Beilstein J. Org. Chem. 12 (2016) 192–197;
(d) T. Pastýříková, G. Iakobson, N. Vida, R. Pohl, P. Beier, Eur. J. Org. Chem. (2012) 2123–2126;
(e) G. Iakobson, P. Beier, Beilstein J. Org. Chem. 8 (2012) 1185–1190;
(f) P. Beier, T. Pastýříková, N. Vida, G. Iakobson, Org. Lett. 13 (2011) 1466–1469;
(g) G. Iakobson, M. Posta, P. Beier, Synlett 24 (2013) 855–859;
(h) N. Vida, P. Beier, J. Fluor. Chem. 143 (2012) 130–134.
[9] (a) T. Okazaki, K.K. Laali, S.D. Bunge, S.K. Adas, Eur. J. Org. Chem. (2014) 1630–1644;
(b) A.S. Reddy, K.K. Laali, Tetrahedron Lett. 56 (2015) 4807–4810.
[10] G. Iakobson, J. Du, A.M.Z. Slawin, P. Beier, Beilstein J. Org. Chem. 11 (2015) 1494–1502.
[11] C. Wang, Y.-B. Yu, S. Fan, X. Zhang, Org. Lett. 15 (2013) 5004–5007.
[12] O.S. Kanishchev, W.R. Dolbier Jr., J. Org. Chem. 81 (2016) 11305–11311.
[13] M.V. Ponomarenko, S. Grabowsky, R. Pal, G.-V. Roschenthaler, J. Org. Chem. 81 (2016) 6783–6791.
[14] B. Duda, D. Lentz, Org. Biomol. Chem. 13 (2015) 5625–5628.
[15] G.A. Olah, G.K.S. Prakash, A. Molnar, J. Sommer, Superacid Chemistry, Wiley,

Hoboken, 2009.
[16] J. Wessel, G. Kleemann, K. Seppelt, Chem. Ber. 116 (1983) 2399–2407.
[17] M.J. Frisch, G.W. Trucks, H.B. Schlegel, G.E. Scuseria, M.A. Robb, J.R. Cheeseman, G. Scalmani, V. Barone, B. Mennucci, G.A. Petersson, et al., Gaussian 09, Revision A.01, Gaussian, Inc, Wallingford, CT, 2009.
[18] (a) A.D. Becke, J. Chem. Phys. 98 (1993) 5648–5652;
(b) C. Lee, W. Yang, R.G. Parr, Phys. Rev. B 37 (1988) 785–789;
(c) B. Miehlich, A. Savin, H. Stoll, H. Preuss, Chem. Phys. Lett. 157 (1989) 200–206.
[19] E.D. Glendening, A.E. Reed, J.E. Carpenter, F. Weinhold, NBO Version 3.1, Gaussian, Inc., Wallingford, CT, 2009.
[20] (a) K. Wolinski, J.F. Hinton, P. Pulay, J. Am. Chem. Soc. 112 (1990) 8251–8260;
(b) R. Dichfield, Mol. Phys. 27 (1974) 789–807.
[21] (a) M.T. Cancès, V. Mennucci, J. Tomasi, J. Chem. Phys. 107 (1997) 3032–3041;
(b) B. Mennucci, J. Tomasi, J. Chem. Phys. 106 (1997) 5151–5158;
(c) B. Mennucci, E. Cancès, J. Tomasi, J. Phys. Chem. B 101 (1997) 10506–10517;
(d) J. Tomasi, B. Mennucci, E. Cancès, J. Mol. Struct. (Theochem.) 464 (1999) 211–226.
[22] F.A. Carey, R.J. Sundberg, Advanced Organic Chemistry, Part A: Structure and Mechanisms, 5th ed., Springer, 2007chapter 9.
[23] (a) H. Shaghaghi, H. Ebrahimi, M. Tafazzoli, M. Jalali-Heravi, J. Fluor. Chem. 131 (2010) 47–52;
(b) H.P. Ebrahimi, M. Tafazzoli, Concepts Magn. Reson. Part A 42A (4) (2013) 140–153.
[24] H. Fukaya, T. Ono, J. Comput. Chem. 25 (2004) 51–60.